ARTICLE

Theoretical Study on Raman Spectra of Aqueous Peroxynitric Acid†

Wen-mei Wei[a], Ren-hui Zheng[b*], Yuan-yuan Jing[b], Ya-ting Liu[a], Jun-cheng Hu[a], Yong Ye[a], Qiang Shi[b*]

a. Department of Chemistry, College of Basic Medicine, Anhui Medical University, Hefei 230026, China

b. Beijing National Laboratory for Molecular Sciences, State Key Laboratory for Structural Chemistry of Unstable and Stable Species, Institute of Chemistry, Chinese Academy of Sciences, Beijing 100190, China

(Dated: Received on October 4, 2011; Accepted on October 14, 2011)

Using density functional theory and polarizable continuum models, we study the Raman spectra of aqueous peroxynitric acid. The calculated results indicate that the solvent effect has significant influence on the electric dipole transition moments between the ground and excited electronic state and Raman polarizabilities. The theoretical Raman spectra agree well with the experimental results. From the experimental depolarization ratio, we can conclude that peroxynitric acid is not a plane molecule. We also find that the hydrogen bond can enhance IR intensity of hydroxyl group by several times.

Key words: Aqueous peroxynitric acid, Raman, Theoretical study

I. INTRODUCTION

Niki *et al.* obtained the first evidence for the existence of peroxynitric acid (PNA/HO_2NO_2) from infrared spectrum in the gas phase in 1977 [1]. Peroxynitric acid HO_2NO_2 is formed in the atmosphere via a three-body recombination reaction involving the HO_2 and NO_2 radicals and a third body M, hence, plays an important role in atmospheric chemistry as a gas-phase temporary reservoir for the odd hydrogen (HO_x) and odd nitrogen (NO_x) families of reactive species in the upper troposphere and lower stratosphere [2, 3]:

$$HO_2+NO_2+M \rightarrow HO_2NO_2+M \quad (1)$$

The dominant atmospheric loss processes for HO_2NO_2 consist of thermal decomposition [4, 5], photodissociation (UV and visible/near-IR) [6−8], and reaction with the OH radical [9]. The contribution of each of these processes to the total loss rate of HO_2NO_2 depends greatly on the location and time [5]. Thermal decomposition of HO_2NO_2 is fast in the lower atmosphere. Above 7 km, however, apart from its reaction with OH, photodissociation constitutes an important removal mechanism for atmospheric HO_2NO_2. The HO_2-NO_2 bond is relatively weak, implying that HO_2NO_2 can be dissociated not only via the absorption of UV photons associated with promotion to a repulsive excited electronic state, but also through unimolecular dissociation initiated by infrared excitation on its ground electronic surface [10, 11]. The latter mechanism is expected to be important. Thus, a thorough understanding of the vibrational and electronic photochemistry is needed.

Kenley *et al.* first prepared peroxynitric acid by reaction of HNO_3 or NO_2BF_4 with H_2O_2, which was identified by IR spectrum [12], and studied the decomposition of peroxynitric acid in aqueous media, and they found that peroxynitric acid decomposes to give molecular oxygen and nitrite. Also, Lammel *et al.* reported the product yield for the decomposition of peroxynitric acid in the pH range from 2 to 7 and nitrite was found to be the dominant product at pH≥5 [13]. Lørgager and Sehested studied peroxynitric acid using pulse radiolysis of oxygenated nitrite and nitrate solutions and determined the formation and decay ratios [14]. Régimbal and Mozurkewich [15] investigated peroxynitric acid decay mechanisms and kinetics at low pH by applying an efficient spectroiodometric method. Experimentally, Appelman and Gosztola obtained the Raman, UV, and ^{15}N NMR spectra of the aqueous peroxynitric acid [16].

Theoretically, the MOLCAS-3 computer code was used by Chen and Hamilton to compute the vertical excitation energies (VEEs) of peroxynitric acid from the complete active space self-consistent field (CASSCF) energies for the first four excited electronic states at the B3LYP/6-31G** optimized ground-state geometry [17]. The CASSCF energy was corrected by second-order perturbation theory (CASPT2 theory) to account for dynamic electron correlation [17]. Li and Francisco calculated the vertical excitation energies for the lowest three excited states of HO_2NO_2 using CASSCF and

†Part of the special issue for "the Chinese Chemical Society's 12th National Chemical Dynamics Symposium".

*Authors to whom correspondence should be addressed. E-mail: zrh@iccas.ac.cn, qshi@iccas.ac.cn

CASPT2 methods [18].

In this work, we calculated the vertical excitation energies for the lowest thirty excited states and the electric dipole transition moments of HO_2NO_2 with the time-dependence density functional theory (TDDFT). Using the ACES II program, Chen and Hamilton also computed the ^{15}N NMR chemical shieldings at the HF and MP2 levels of theory for peroxynitric acid [17]. However, the theoretical Raman spectra for peroxynitric acid in liquid phase have not been reported. Raman and IR are vibrational spectra and directly related to molecule structure. In aqueous phase, peroxynitric acid decomposes to form products different from those in the gas phase [13]. Peroxynitric acid in aqueous solution is of particular interest for atmospheric processes involving aerosol and cloud water chemistry. Thus, in this work, we also calculated the Raman and IR spectra of HO_2NO_2 in gas phase and liquid phase, and the forming of hydrogen bond with water.

II. THEORY AND COMPUTATIONAL METHOD

Using the density functional method [19, 20] B3LYP and the split valence polarized basis set 6-311++G** with Gaussian 09 program [21], we perform a geometry optimization and calculate the fundamental frequencies for peroxynitric acid. Then Hessian matrix of force constants and frequency-dependent polarizabilities derivative with respect to Cartesian coordinate are obtained. By diagonalizing the Hessian matrix we obtain the transformation matrix between the normal coordinate and Cartesian coordinate. Utilizing this transformation matrix we get Raman components for all vibrational modes. According to the Raman definition [22], we calculate the Placzek isotropic, anisotropy tensor invariants, depolarization ratio, the differential scattering cross-sections with the scattered radiation polarized parallel and perpendicular to the polarization of the incoming beam, and total Raman scattering cross-section. The IR activities have also been computed. On the basis of optimization, TDDFT is applied to compute the excited electronic singlet states and electric dipole transition moments [23, 24]. We take the solvation effect into account with polarizable continuum models (PCM) method [25−27].

III. RESULTS AND DISCUSSION

A. Ground state

The ground electronic state of peroxynitric acid is C_1 symmetry with the hydrogen nearly orthogonal to the plane formed by the other atoms (see Fig.1(a)). This agrees with the results obtained by Chen *et al.* who applied a high-level *ab initio* theoretical study [17]. The molecular structure and symmetry determine the IR and Raman activities and Raman depolarization ratio. When the molecule is C_1 symmetry, all the vibrational modes are both IR and Raman activities. We also study the solvent effect of HO_2NO_2 in water using PCM and forming a hydrogen bond with a water molecule (see Fig.1(b)). The solvent effect influences the molecule structure. In vacuum, the bond length of O2−N4 bond is 1.531 Å, which are 1.518 Å in solvent and 1.509 Å forming a hydrogen bond. In water solvent, the O2−N4 bond becomes a little shorter. The O2−N4 bond is the weakest bond among the HO_2NO_2 molecule. The solvent effect makes this bond a little stronger. From Table I, we also see that the hydrogen bond affects the O1−H3 bond, which are 0.972 Å in vacuum and 0.985 Å with a hydrogen bond. The bond length becomes longer and it may be easier for the hydrogen of HO_2NO_2 to ionize in water solvent. Furthermore, the solvent effect impacts on bond angles and dihedral angles. The vibrational frequencies, IR and Raman intensities depend on the molecule structure and the interaction of molecule with solvent. Thus, the IR and Raman spectra in vacuum are different from those in water solvent.

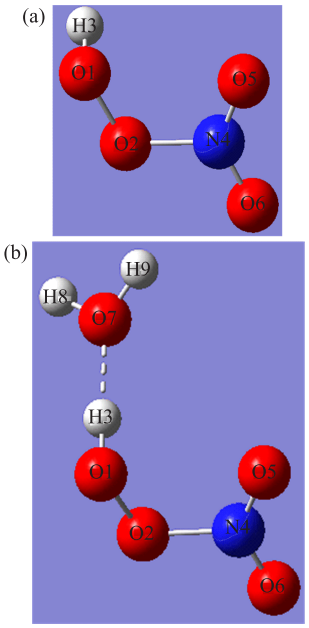

FIG. 1 Molecular structure of peroxynitric acid in gas phase (a) and in water (b).

B. Excited state

Based on the optimization, we calculate properties of the excited states. The excited energies, electric dipole transition moments, and oscillator strengths of HO_2NO_2 for the first 30 electronic states in vacuum are listed in Table II and those in water are in Table III. All the excited states are A symmetry due to the molecular C_1 symmetry. The excited energies of the four excited

DOI:10.1088/1674-0068/24/05/625-630

TABLE I The properties of bond length R (in Å), bond angles A and dihedral angles D (in °) of HO_2NO_2 used in gas and water, and forming hydrogen bond with water.

	Gas	Water	Forming hydrogen bond
R(O1−O2)	1.399	1.398	1.398
R(O1−H3)	0.972	0.974	0.985
R(O2−N4)	1.531	1.518	1.509
R(H3−O7)			1.764
R(N4−O5)	1.189	1.187	1.192
R(N4−O6)	1.190	1.193	1.194
R(O7−H8)			0.963
R(O7−H9)			0.963
A(H3O1O2)	103.4	103.4	103.2
A(O1O2N4)	109.6	110.0	110.1
A(O1H3O7)		179.1	
A(O2N4O5)	116.4	117.0	116.9
A(O2N4O6)	109.9	109.7	110.4
A(O5N4O6)	133.8	133.3	132.7
A(H3O7H8)			125.1
A(H3O7H9)			122.3
A(H8O7H9)			106.9
D(H3O1O2N4)	90.3	93.4	86.8
D(O2O1H3O7)		10.6	
D(O1O2N4O5)	−9.7	−4.9	−8.4
D(O1O2N4O6)	171.1	175.1	172.5
D(O1H3O7H8)			88.4
D(O1H3O7H9)			−121.7

states are 4.9781, 5.3016, 5.8161, and 6.6231 eV, respectively. Chen *et al.* computed the corresponding vertical excited energies which are 4.903, 5.171, 5.853, and 7.009 eV by CASPT2 and 5.041, 5.433, 6.468, and 7.535 eV by CAS, respectively [17]. The results of the first three excited states agree well with each other. And the difference of the four excited state between TD, CASPT2 and CAS are a little larger. Due to A symmetry, all the excited states are electric dipole transition allowed. In vacuum, the oscillator strengths of the first two excited states are about 0.0000 and 0.0001, respectively. This indicates these two excited states can hardly absorb photon. The oscillator strength of the third excited state is a little larger with the value of 0.0055. The largest oscillator strength among the 30 excited states is 0.1697 of the 16th excited state with an excited energy of 9.0408 eV, which indicates that peroxynitric acid in atmosphere can absorb UV light strongly. Using PCM, we also study the excited states in water solvent. The solvent effect has little influence on the excited energies but much influence on the electric dipole transition moments (oscillator strengths). For example, in water the largest oscillator strength is also from the 16th excited state and can be 0.2552; and the y component of the transition moment for the first excited

TABLE II Calculated excited energies (in eV), electric dipole transition moments x, y, z (in a.u.), oscillator strength f of HO_2NO_2 in vacuum using TDDFT//B3LYP/6-311++G** method.

State	Energy	x	y	z	f
1A	4.9781	0.0119	0.0097	−0.0046	0.0000
2A	5.3016	−0.0176	0.0108	−0.0133	0.0001
3A	5.8161	0.1954	−0.0235	0.0046	0.0055
4A	6.6231	−0.0151	0.0898	−0.0307	0.0015
5A	6.8276	0.1987	−0.3226	−0.0102	0.024
6A	7.1089	0.2982	−0.0624	0.0007	0.0162
7A	7.1493	0.225	−0.0516	0.0437	0.0097
8A	7.3883	−0.1328	0.0604	0.1349	0.0071
9A	7.4738	−0.5231	0.0152	−0.0505	0.0506
10A	7.5600	0.1765	−0.0363	0.0228	0.0061
11A	8.1821	−0.4444	−0.5847	−0.0178	0.1082
12A	8.2050	0.2713	0.3844	−0.0103	0.0445
13A	8.3632	−0.4149	−0.0998	−0.0896	0.039
14A	8.5093	−0.4127	0.3546	0.0283	0.0619
15A	8.6745	−0.085	0.0989	−0.1009	0.0058
16A	9.0408	0.8724	−0.0572	0.0414	0.1697
17A	9.3410	−0.2914	0.3711	−0.0007	0.051
18A	9.4285	0.5169	−0.1794	−0.035	0.0694
19A	9.5473	0.2467	−0.4881	0.0295	0.0702
20A	9.6709	0.0253	0.0424	−0.0252	0.0007
21A	9.9785	0.7822	−0.063	0.0034	0.1505
22A	10.1055	−0.1161	−0.0127	−0.0838	0.0051
23A	10.3384	−0.0312	0.1846	−0.0691	0.0101
24A	10.5113	0.0279	−0.4291	−0.0063	0.0476
25A	10.5870	0.1795	0.0894	−0.0369	0.0108
26A	10.6534	0.0648	−0.0146	0.0716	0.0025
27A	10.7156	0.012	0.1799	−0.0154	0.0086
28A	10.8050	−0.4297	−0.2043	−0.017	0.06
29A	10.9313	−0.0215	−0.0422	−0.1179	0.0043
30A	11.0082	0.2099	−0.2208	0.0785	0.0267

state is 0.0131, which is 35% larger than that in vacuum. The water is a polar molecule and impacts on the electric dipole transition moments. As we know, one method to obtain the Raman polarizability is sum-over excited states, which relates the Raman polarizability to photon frequency, excited energies, and transition moments. Thus we deduce that the Raman polarizability should also be changed largely under the influence of the water solvent.

C. Raman spectra

Raman is a vibrational spectroscopy, which includes non-resonant Raman and resonant Raman. Both can be applied to detect molecular structure. Resonant Raman is also used to study the structure of the excited

DOI:10.1088/1674-0068/24/05/625-630

TABLE III Calculated excited energies (in eV), electric dipole transition moments x, y, z (in a.u.), oscillator strength f of HO_2NO_2 in water using TDDFT//B3LYP/6-311++G** method with polarizable continuum (PCM) models in water solvent.

State	Energy	x	y	z	f
1A	5.0101	−0.0230	0.0131	−0.0032	0.0001
2A	5.3092	−0.0302	0.0127	−0.0106	0.0002
3A	5.8218	0.2744	−0.0436	0.0034	0.0110
4A	6.7531	0.1469	−0.0157	−0.0285	0.0037
5A	6.8834	−0.1943	0.4197	−0.0031	0.0361
6A	7.0591	0.0238	−0.0165	0.0438	0.0005
7A	7.2064	−0.5726	0.0359	−0.0003	0.0581
8A	7.5759	0.1672	0.0226	0.1149	0.0077
9A	7.6773	−0.0323	−0.0045	0.0192	0.0003
10A	7.7532	−0.6458	−0.1159	0.0156	0.0818
11A	8.1676	0.3583	0.8373	−0.0110	0.1660
12A	8.5240	0.0560	−0.0091	−0.0321	0.0009
13A	8.6913	−0.2934	0.2219	0.0621	0.0296
14A	8.7526	−0.4353	0.0089	−0.0847	0.0422
15A	9.0003	−0.0060	−0.0060	−0.1079	0.0026
16A	9.0865	1.0528	−0.1931	0.0239	0.2552
17A	9.3894	0.4895	0.0040	−0.0209	0.0552
18A	9.5410	−0.3769	0.5170	0.0298	0.0959
19A	9.8070	−0.0324	−0.3938	0.0080	0.0375
20A	9.8558	0.0566	0.0222	−0.0297	0.0011
21A	10.0025	0.8170	−0.1189	0.0050	0.1670
22A	10.1292	0.0349	−0.0316	−0.0760	0.0020
23A	10.4723	0.0369	0.2831	−0.0321	0.0212
24A	10.5254	0.0201	−0.5038	0.0187	0.0656
25A	10.5993	0.0040	0.0730	−0.0643	0.0025
26A	10.7011	0.2268	−0.0394	0.0715	0.0152
27A	10.7392	0.3391	0.0575	−0.0462	0.0317
28A	10.8129	−0.0266	0.0184	−0.1600	0.0071
29A	10.8543	0.3897	0.1006	−0.0053	0.0431
30A	10.9930	0.0582	−0.2863	0.0062	0.0230

states. Appelman *et al.* have studied Raman spectra of aqueous peroxynitric acid experimentally [16], which is a non-resonant Raman with an excited photon frequency of 514.5 nm. We calculate Placzek isotropic and anisotropy tensor invariants, total Raman scattering activities and the depolarization ratio in vacuum and water solvent (Table IV). The computed Raman spectra with the polarization of the scattered light parallel and perpendicular to incident light are shown in Fig.2. The calculated spectra are in the unit of A^4/amu, but the experimental Raman spectra only have relative intensities. In order to compare the results of the theory with that of the experiment, we take their most intense peaks to be the same in water solvent (Fig.3). In experiment, the 1301 cm^{-1} mode is the second strongest Raman mode and its parallel intensity is about 87%

TABLE IV Calculated vibrational frequencies F (in cm^{-1}) scaled by a factor of 0.9614, Placzek isotropic and anisotropy tensor invariants Σ^0, and Σ^2, total Raman scattering activities $d\sigma/d\Omega$ (in A^4/amu) and the depolarization ratio ρ by B3LYP/6-311++G** and PCM. And experimental Raman vibrational frequencies and depolarization ratio are also listed.

F	Σ^0	Σ^2	$d\sigma/d\Omega$	ρ	F^a	ρ^a
142	0.0006	0.7768	0.3884	0.7486		
303	2.3851	5.3169	3.9164	0.3535		
385	1.8393	2.9045	1.5254	0.2903	340	0.4481
440	21.5286	37.3644	27.8559	0.3073	483	0.3475
630	1.2775	16.5535	7.4011	0.6287	654	0.9202
709	0.0462	0.2765	0.1615	0.5291		
768	10.3157	6.0558	9.0388	0.1426	805	0.2000
954	6.1582	6.6291	6.5736	0.2257	945	0.1583
1287	19.2859	19.8441	14.0881	0.2187	1301	0.1718
1371	2.6783	13.4496	10.0058	0.5007		
1691	0.1992	18.4547	6.4003	0.7303	1707	0.6744
3556	71.7947	72.2173	94.9913	0.2152		

[a] Data from Ref.[16].

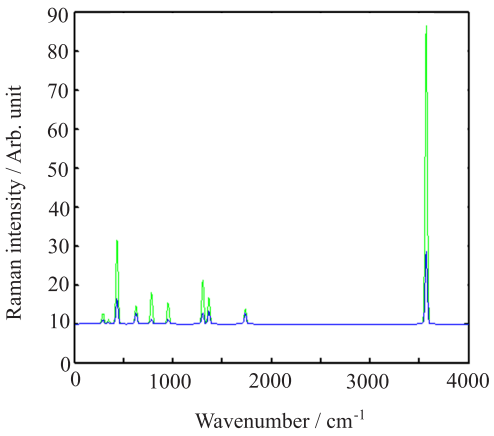

FIG. 2 Calculated Raman spectra with the polarization of the scattered light parallel (green line) and perpendicular (blue line) to that of the exciting light.

as large as the most intense peak, however, the calculated value is 13 A^4/amu and only 52% as large as the most intense peak, which underestimates this Raman band. The reason may be that the solvent effect has not been taken into consideration. In Fig.3, we plot parallel and perpendicular Raman spectra in water solvent using PCM models. From Fig.3, we can see that the theoretical and experimental spectra agree with each other. In this case, the intensity of the 1301 cm^{-1} is enhanced much and can be 88% as large as the most intense peak. Comparing Fig.2 and Fig.3, we find that the Raman intensities become larger in solvent. For example, the most intense peak is the 432 cm^{-1} mode with

DOI:10.1088/1674-0068/24/05/625-630

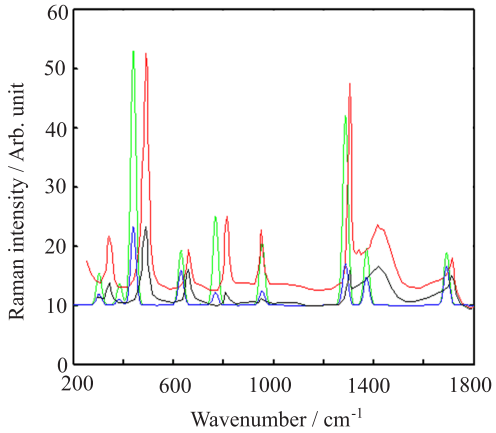

FIG. 3 Calculated parallel (green line) and perpendicular (blue line) Raman spectra in water solvent using PCM models. And the experimental parallel (red line) and perpendicular (black line) Raman spectra are from Ref.[16].

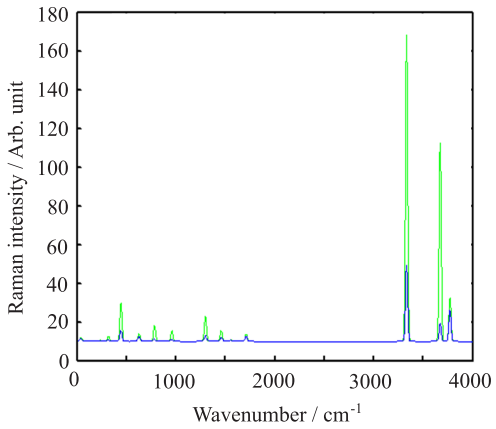

FIG. 4 Calculated parallel (green line) and perpendicular (blue line) Raman spectra for HO_2NO_2 and H_2O supramolecule.

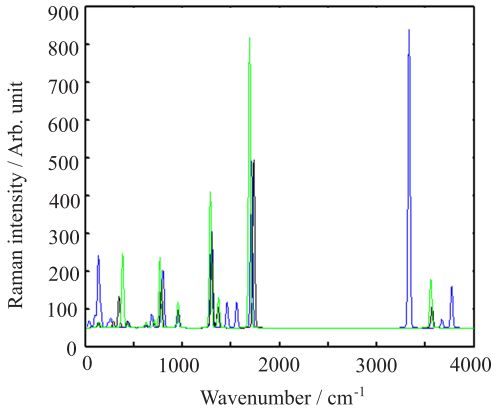

FIG. 5 Calculated IR spectra of HO_2NO_2 in vacuum (black line), in water solvent using PCM models (green line), and HO_2NO_2 and H_2O supramolecule (blue line).

a parallel intensity of 21 A^4/amu in vacuum and that is 42 A^4/amu in water. The solvent effect can make this Raman peak enhance twice. Peroxynitric acid and water are both polar molecules, and the electronic cloud of Peroxynitric acid may be changed much in the presence of water molecules. This change influences the electric dipole moment, electric dipole transition moments and Raman polarizabilities. The x, y, and z components of electric dipole moments of the ground state are respectively 1.3665, 0.5689, and 1.6004 Debye in vacuum and those are 1.7939, 0.4886, and 1.9398 Debye in water. The large difference in dipole moments induces large difference in Raman polarizabilities.

Now we turn to discuss the depolarization ratio. As we know, if all the atoms of HO_2NO_2 are in the same plane, HO_2NO_2 belongs to C_s symmetry, which has vibrational modes with A′ and A″ symmetry. The depolarization ratio of the non-symmetric A″ modes should be 0.75. However, in experiment scientists did not observe this phenomenon. This indicates HO_2NO_2 is not a plane molecule in gas phase and in water solvent. Previous optimization shows that the hydrogen atom is nearly orthogonal to the plane of the other atoms. Another interesting thing of the depolarization ratio is that abnormal value of the 654 cm^{-1} mode. The depolarization ratio of this mode can be as large as 0.9202 experimentally, which is much larger than 0.75. Just as we know, if there is no antisymmetric polarizability, the depolarization ratio must be smaller than 0.75. Generally in non-resonant case, the antisymmetric polarizability can be two orders of magnitude smaller than symmetry one [28−31]. Thus non-resonant antisymmetric polarizability almost does not influence the depolarization ratio. However, the value 0.9202 of this Raman experiment indicates that the antisymmetric polarizability can be the same order of magnitude of the symmetric one in non-resonant case. Only in resonant case, the antisymmetric polarizability can be so large. If the experiment is correct, the reason of abnormal depolarization ratio needs to be studied further.

D. Raman and IR of HO_2NO_2 with a water molecule

In order to study the Raman and IR spectra under the influence of hydrogen bond with water molecule, we calculate the spectra of HO_2NO_2 and H_2O supramolecule. The Raman spectra are plotted in Fig.4. When there is a hydrogen bond between HO_2NO_2 and H_2O, the HO vibrational frequency of HO_2NO_2 is red-shifted to 3466 cm^{-1} with a Raman activity of 166 A^4/amu, which is 144 A^4/amu using PCM and 81 A^4/amu in vacuum, respectively. The hydrogen bond makes Raman activity twice larger. The IR spectra have also been studied, which are plotted in Fig.5. The IR intensities are 789 km/mol forming hydrogen, 128 km/mol using PCM and 57 km/mol in vacuum, respectively.

DOI:10.1088/1674-0068/24/05/625-630

The IR intensity of HO vibrational mode of HO_2NO_2 forming hydrogen bond can be 13.8 times as large as that in vacuum. The hydrogen bond enhances IR intensity much. This phenomenon also exists when the IR spectra of water and methanol in liquid phase were investigated [32, 33].

IV. CONCLUSION

Applying density functional theory and polarizable continuum models, we optimize the structure of the ground state for peroxynitric acid in water and calculate Raman spectra. The solvent effect impacts much on Raman intensity. And the calculated spectra agree well with experiment. Based on the optimization, using TDDFT we compute the excited states, which generally agree with those from high-level theory. And the electric dipole transition moments change much under the influence of the solvent effect. The influence of IR intensity of hydroxyl group by the hydrogen bond is also investigated. The hydrogen bond makes IR intensity of hydroxyl group much stronger.

V. ACKNOWLEDGMENTS

This work was supported by the National Natural Science Foundation of China (No.20903101 and No.21103003).

[1] H. Niki, P. D. Maker, C. M. Savage, and L. P. Breitenbach, Chem. Phys. Lett. **45**, 564 (1977).
[2] G. Brasseur, J. J. Orlando, and G. S. Tyndall, *Atmospheric Chemistry and Global Change*, Oxford: Oxford University Press, (1999).
[3] R. J. Salawitch, P. O. Wennberg, G. C. Toon, B. Sen, and J. F. Blavier, Geophys. Res. Lett. **29**, 1762 (2002).
[4] F. Zabel, Z. Phys. Chem. (Muenchen) **188**, 119 (1995).
[5] T. Gierczak, E. Jiménez, V. Riffault, J. B. Burkholder, and A. R. Ravishankara, J. Phys. Chem. A **109**, 586 (2005).
[6] E. Jiménez, T. Gierczak, H. Stark, J. B. Burkholder, and A. R. Ravishankara, Phys. Chem. Chem. Phys. **7**, 342 (2005).
[7] C. M. Roehl, S. A. Nizkorodov, H. Zhang, G. A. Blake, and P. O. Wennberg, J. Phys. Chem. A **106**, 3766 (2002).
[8] J. Matthews, R. Sharma, and A. Sinha, J. Phys. Chem. A **108**, 8134 (2004).
[9] E. Jiménez, T. Gierczak, H. Stark, J. B. Burkholder, and A. R. Ravishankara, J. Phys. Chem. A **108**, 1139 (2004).
[10] D. J. Donaldson, G. J. Frost, K. H. Rosenlof, A. F. Tuck, and V. Vaida, Geophys. Res. Lett. **24**, 2651 (1997).
[11] D. J. Donaldson, A. F. Tuck, and V. Vaida, Phys. Chem. Earth C **25**, 223 (2000).
[12] R. A. Kenley, P. L. Trevor, and B. Y. Lan, J. Am. Chem. Soc. **103**, 2203 (1981).
[13] G. Lammel, D. Perner, and P. Warneck, J. Phys. Chem. **94**, 6141 (1990).
[14] T. Lørgager and K. Sehested, J. Phys. Chem. **97**, 10047 (1993).
[15] J. M. Régimbal and M. Mozurkewich, J. Phys. Chem. A **101**, 8822 (1997).
[16] E. H. Appelman and D. J. Gosztola, Inorg. Chem. **34**, 787 (1995).
[17] Z. Chen and T. P. Hamilton, J. Phys. Chem. **100**, 15731 (1996).
[18] Y. Li and J. S. Francisco, J. Chem. Phys. **114**, 211 (2001).
[19] C. Lee, W. Yang, and R. G. Parr, Phy. Rev. B **37**, 785 (1988).
[20] A. D. Becke, J. Chem. Phys. **98**, 5648 (1993).
[21] M. J. Frisch, G. W. Trucks, H. B. Schlegel, G. E. Scuseria, M. A. Robb, J. R. Cheeseman, G. Scalmani, V. Barone, B. Mennucci, G. A. Petersson, H. Nakatsuji, M. Caricato, X. Li, H. P. Hratchian, A. F. Izmaylov, J. Bloino, G. Zheng, J. L. Sonnenberg, M. Hada, M. Ehara, K. Toyota, R. Fukuda, J. Hasegawa, M. Ishida, T. Nakajima, Y. Honda, O. Kitao, H. Nakai, T. Vreven, J. A. Montgomery Jr., J. E. Peralta, F. Ogliaro, M. Bearpark, J. J. Heyd, E. Brothers, K. N. Kudin, V. N. Staroverov, R. Kobayashi, J. Normand, K. Raghavachari, A. Rendell, J. C. Burant, S. S. Iyengar, J. Tomasi, M. Cossi, N. Rega, J. M. Millam, M. Klene, J. E. Knox, J. B. Cross, V. Bakken, C. Adamo, J. Jaramillo, R. Gomperts, R. E. Stratmann, O. Yazyev, A. J. Austin, R. Cammi, C. Pomelli, J. W. Ochterski, R. L. Martin, K. Morokuma, V. G. Zakrzewski, G. A. Voth, P. Salvador, J. J. Dannenberg, S. Dapprich, A. D. Daniels, O. Farkas, J. B. Foresman, J. V. Ortiz, J. Cioslowski, and D. J. Fox, *Gaussian 09, Revision A.02*, Wallingford CT: Gaussian, Inc., (2009).
[22] O. S. Mortensen and S. Hassing, Adv. Infrared Raman Spectrosc. **6**, 1 (1980).
[23] R. Bauernschmitt and R. Ahlrichs, Chem. Phys. Lett. **256**, 454 (1996).
[24] M. E. Casida, C. Jamorski, K. C. Casida, and D. R. Salahub, J. Chem. Phys. **108**, 4439 (1998).
[25] S. Miertus, E. Scrocco, and J. Tomasi, Chem. Phys. **55**, 117 (1981).
[26] S. Miertus and J. Tomasi, Chem. Phys. **65**, 239 (1982).
[27] M. Cossi, V. Barone, R. Cammi, and J. Tomasi, Chem. Phys. Lett. **255**, 327 (1996).
[28] F. C. Liu, J. Phys. Chem. **95**, 7180 (1991).
[29] M. A. Belkin, T. A. Kulakov, K. H. Ernst, L. Yan, and Y. R. Shen, Phys. Rev. Lett. **85**, 4474 (2000).
[30] M. A. Belkin, Y. R. Shen, and R. A. Harris, J. Chem. Phys. **120**, 10118 (2004).
[31] R. H. Zheng and W. M. Wei, J. Phys. Chem. B **111**, 1431 (2007).
[32] B. M. Auer and J. L. Skinner, J. Chem. Phys. **128**, 224511 (2008).
[33] R. H. Zheng, Y. Y. Sun, and Q. Shi, Phys. Chem. Chem. Phys. **13**, 2027 (2011).

DOI:10.1088/1674-0068/24/05/625-630